Received: 21 November 2019 Accepted: 12 February 2020 *DOI ID: 10.5505/jems.2020.84803*

Journal of ETA Maritime Science

JEMS JOURNAL

Corresponding Author: Hüseyin ELÇİÇEK

TC-UV Reactors Evaluated as an Alternative Option in Treatment of Ballast Water

Hüseyin ELÇİÇEK[1], Bülent GÜZEL[1]

[1]Yıldız Technical University, Faculty of Naval Architecture and Maritime, Turkey
helcicek@gmail.com; ORCID ID: https://orcid.org/0000-0003-1064-6668
bguzel@yildiz.edu.tr; ORCID ID: https://orcid.org/0000-0001-6915-4209

Abstract

Over the last decade, UV disinfection technology has been widely employed in the disinfection of non-native species in wastewater and process water treatment. In this study, we assessed the feasibility of the adoption of a Taylor-Couette UV reactor in disinfection of unwanted species commonly found in ballast water. With this purpose, glycerol solutions were used in a Taylor Couette reactor with two different radius ratios. The observed flow structures and the critical transition values were simultaneously compared with each other and literature. Emergent flow structures in TC reactors provide considerable improvement in axial and radial mixing of particles and increasing the efficiency of the disinfection of E. coli. The obtained results show the possibility of utilizing the Taylor-Couette UV reactors as an alternative method in inactivation of non-native species in the ballast water.

Keywords: *Taylor Couette flow, Ballast water, UV disinfection.*

To cite this article: Elçiçek, H. & Güzel, B. (2020). TC-UV Reactors Evaluated as an Alternative Option in Treatment of Ballast Water. *Journal of ETA Maritime Science*, 8(1), 10-21.
To link to this article: https://dx.doi.org/10.5505/jems.2020.84803

1. Introduction

Maritime traffic worldwide has significantly increased with the globalized economy and the international trade system. This rapid development in maritime transport has resulted in an increased amount of released harmful pollutants into the marine environment, such as oily bilge water, garbage, sewage, ballast water and tank washings [1]. These pollutants endanger marine life and influence the coastal environment, and significantly affect human health. Among them, ballast water is one of the most dangerous threats to the marine environment. Tens of foreign species are discharged into the marine environment via ships each period, and these species can lead to significant changes to the structure of marine ecosystems and extensive coastal destruction. They are also considered to be a potential threat to human health [2,3].

In order to prevent introducing invasive species into the seas, a global protocol (Ballast Water Management Convention) for controlling and managing ballast water and sediments coming from ships has been adopted by IMO [4]. Under the rules of BWMC, the available techniques used in ballast water treatment can be listed as the systems of ultraviolet (UV) irradiation, electrolysis, ozonation, mechanical and chemical filtration. Each of these treatment options has its own advantages and disadvantages. For example, while the electrolytic disinfection and biocide processes are accepted as an effective treatment method, they lead to considerable corrosion losses from the ballast tanks and generation of undesirable by-products and effluents resulting from the chemical reactions. On the other hand, the UV disinfection process is a well-known chemical-free process that does not generate any harmful by-products and has many other advantages. This method is already used in inactivation of various microbial pathogens contained in the ballast water [5–7] as one of the most widely preferred disinfection methods (~48%) in the ballast water treatment technologies [8]. Previous studies on UV disinfection processes have mainly focused on minimizing and mitigating the introduction of invasive species via ballast water. Among them, Wu et al. (2011) compared the efficiency of UV and UV+ozone (O3) processes in disinfecting *E. coli* (indicator microorganism) in ballast water. Their results showed that the combined treatment of UV+ozone was significantly more effective in reducing indicator microorganisms than the UV unit used alone [9]. Monroy et al. (2018) investigated the disinfection efficiency of a treatment unit, including UV-C process and mechanical filter at different temperatures. It is reported that UV-C irradiation has a higher inactivation efficiency at low temperatures [10]. Lu et al. (2018) investigated the use of a high-gradient magnetic separation UV titanium-oxide photocatalysis system to inactivate *E. coli* in ballast water. Their results have indicated that the proposed disinfection technology can be effectively used to inactivate *E. coli* in ballast water [11]. Jung et al. (2012) studied the efficiency of medium-pressure ultraviolet (MPUV) treatment unit for reducing several indigenous marine species in ballast water. They reported that when a combination of the filtration and the MPUV irradiation was applied, inactivation percentages of the tested organisms were achieved to be above 99.99% [12].

The previous studies showed that the UV irradiation is still one of the most widely used methods in ballast water treatment. Therefore, future efforts are to focus on improving the efficiency and the performance of the UV irradiation techniques. Recent studies show that Taylor-Couette UV (TC-UV) reactors have been used effectively as an alternative

disinfection method for various fluids [13–17] in different industries. For more than a century, Taylor-Couette flows have been studied in fluid mechanics at a fundamental level, e.g. in proving the no-slip boundary condition and the Navier-Stokes equations describing the Newtonian fluid flow. Taylor-Couette flows are already used in different industries. The efficiency of rotating filter separators used in separation and filtration of suspensions is much higher than those of other filtration methods, due to a much thinner cake formation on the filter under radial flow effects. Because the centrifugal instability in Taylor–Couette flows during supercritical transition increases the axial and radial dispersion via nonwavy and wavy toroidal vortices [18]. Taylor-Couette flows occur between independently rotating coaxial cylinders, and more than 26 different flow states may exist in Taylor-Couette flows between counter-rotating cylinders for a radius ratio of 0.88 [19]. Rudman (1998) carried dye tracer experiments and determined axial dispersion coefficients via DNS simulations, and showed that these mixing characteristics depend on the azimuthal wavelength and number in the wavy flow [20]. Whereas, low axial mixing in TVF increase high separation efficiency in case of liquid–liquid extraction applications. With increasing the rotational speed of the inner cylinder, the toroidal vortices carry azimuthal momentum radially within the annular gap. When the flow becomes WVF with wavy vortices, the fluid particles is transferred axially between the adjacent vortices. Therefore, WVF flow provides significant contributions to the mixing of particles [21]. In this regime, the vortex centers move axially and radially. Thus, the vortices formed in the TC-UV reactors may provide effective radial and axial mixing with higher values of heat and mass transfer coefficients.

Moreover, the thickness of the cake layers occurred between fluid and the UV source is reduced, providing prolonged UV exposure periods for the invasive species and uniform radiation levels [14,22,23]. Forney et al. (2008) studied the effect of boundary layer and wavy walls on the inactivation efficiency of *E. coli* using concentric cylinders. They indicated that higher axial velocities with longer cylinders are required for inactivating *E. coli* at the turbulent flow. And, the inactivation of microorganisms was increased with the wavy wall modifications in TC flows [21]. Ye et al. (2008) determined the optimum disinfection efficiency of microbes in various flow conditions. Their results show that inactivation in the laminar Taylor Couette flow was found to have significantly higher efficiency compared to the inactivation at laminar Poiseuille or turbulent flow. They also indicated that the flow structure is one of the most important indicators to determine disinfection efficiency [22]. Orlowska et al. (2014) tested the performance of a pilot-scale TC-UV reactor for inactivation of *E. coli* at various flow conditions. They show that inactivation of *E. coli* is entirely dependent on the Reynolds numbers, and the flow regimes occurred in the gap. The results have also demonstrated that the microbial inactivation efficiency was decreased at Couette–Poiseuille (CP) flow relative to that at turbulent vortices (TV) [23].

Previous studies investigating the disinfection of microbial species in TC-UV reactors are primarily in the food industry. It is known that the emergent flow structures in TC-UV reactors are significant in improving the inactivation process of microorganisms. The flow structures formed in the annular gap and their critical transition values are unexplored in terms of UV disinfection efficiency in the marine industry. This study aims to develop a comprehensive understanding of the emergent secondary flows in TC reactors

for improving the efficiency levels of the ballast water treatment. In this regard, the effect of the radius ratio and the inner cylinder Reynolds number (Re_i) on the secondary fluid flows were investigated through various values of the rotational rate of the inner cylinder. The experiments were conducted to determine the critical Reynolds number at which the secondary bifurcation in a TC reactor occurs and their effect on the treatment efficiency.

2. Materials and Methods

The Taylor-Couette setup used for the experiments in this study consists of two concentric cylinders and shown schematically in Fig. 1. The geometrical specifications of the TC setup and its characteristic dimensionless parameters are listed in Table 1. In order to examine the effect of the radius ratio on flow bifurcation, two different cylinder diameters were used in this study. Both the inner and outer cylinders can be rotated independently in the range of 5–300 rpm in order to reach the desired Reynolds number values after transition and compare the flow patterns. The rotation speed of the cylinders slowly varied. The inner cylinder is made of aluminium, and its surface is uniformly coated with black acrylic paint. The outer cylinder is made of transparent plexiglass to

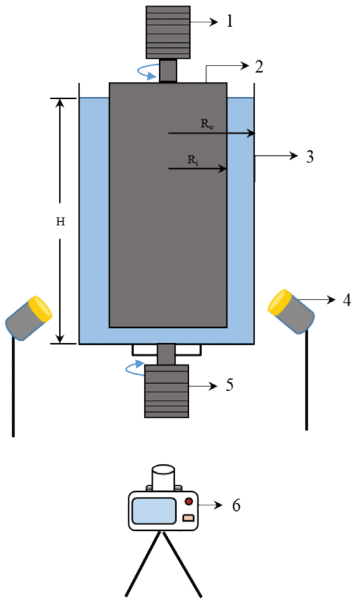

1 – DC motor (controlling inner cylinder)
2 – Inner cylinder
3 – Outer cylinder
4 – Light source
5 – DC motor (controlling outer cylinder)
6 – High–speed camera

Figure 1. *Schematic View of the Experimental Setup*

Table 1. *Geometrical Specifications of the Cylinders and the Dimensionless Parameters*

Parameters	Abbreviation	Value used in the experiments
Outer cylinder radius [mm]	R_o	72 and 70
Inner cylinder radius [mm]	R_i	62.5 and 45
Active column height [mm]	H	400
Gap [mm]	d	9.5 and 25
Radius ratio	η	0.868 and 0.643
Aspect ratio	Γ	~42 and 16

obtain better visualization. The rotational rate of the inner cylinder is measured using an optical tachometer.

Two different concentrations of glycerol solutions were used as a working fluid. The rheological properties of the test fluids used in the experiments are presented in Table 2. Dynamic viscosity of the working fluids was determined using a rheometer by Anton Paar, MCR 302. The viscosity measurements were performed in a water bath controlled with a Peltier system and repeated at least three times for each solution. The precision in viscosity measurements was about ±0.5%. A reflective digital tachometer with an accuracy of ±0.05% was used to measure the rotational rate of the inner cylinder. The emergent flow patterns in the gap have been visualized using reflective flakes. These particles have unique properties that they align themselves with the direction of the flow, and their contrast reflection makes it possible to visualize the various flow structures. Flow visualizations were recorded at a rate of 200 fps by a high-speed CCD camera (Phantom Miro eX4) with 800×600 pixel resolution. The acquired images from the experiments were then enhanced via post-processing by adjusting the brightness and contrast.

Table 2. *Rheological Properties of the Glycerol Solutions Used in Experiments*

Solution	ρ [kg/m^3]	μ [Ns/m^2]
Glycerol 60 wt%	1148	0.0096
Glycerol 75 wt%	1187	0.028

For a Newtonian fluid flow between concentric cylinders, the Reynolds number, Re for a system with the inner cylinder rotating only is the inner Reynolds number, Re_i and defined as;

$$\mathrm{Re}_i = \frac{\rho \omega_i R_i d}{\mu} \tag{1}$$

where ρ is the fluid density, R_i is the inner cylinder radius, ω_i is the rotational speed of the inner cylinder, and μ is the fluid viscosity. In this system, the azimuthal flow is forced by rotating the inner cylinder at the desired rate. The critical conditions of the primary and secondary flow transitions are defined by the critical Reynolds number, Re_c.

In this study, the inactivation ratio was calculated for *E. coli* inactivation in ballast waters and follows the first-order kinetics, and given by

$$\frac{N}{N_0} = \exp(-k \times E) \tag{2}$$

In Eqn. 2, N is surviving population after exposure to UV influence (CFU/mL), N_0 is the initial concentration of *E. coli* (CFU/mL), k is first-order inactivation constant (cm^2/mJ), E is UV influence (mJ/cm^2).

The Lambert-Beer's law was used to determine the UV irradiance distribution in the annular gap. If the UV lamps are placed inside the inner cylinder, the UV irradiance distribution can be calculated using Eqn. 3 [24]. The general UV light irradiance (I) within the annular gap is obtained using Eqn. 4 [23].

$$I(r) = I_0 \frac{R_i}{r} \exp(-\alpha(r - R_i)) \tag{3}$$

$$I = \frac{I_0}{\alpha d}\left[1 - \exp(-\alpha d)\right] \tag{4}$$

where α is the absorbance coefficient (cm^{-1}), and I_0 is UV irradiance at the surface of the UV source. Then, the inactivation rate for a TC reactor can be defined as follows;

$$\ln\left(\frac{N}{N_0}\right) = -\frac{k I_0 \tau R_c}{\alpha d} \qquad R_c = \frac{2R_i}{R_o + R_i} \tag{5}$$

The absorption coefficient was taken as α=0.5 cm^{-1}, and UV doses were applied in the range of 5 to 25 mJ/cm^2.

3. Results and Discussion

In the present work, the critical transition values and the flow patterns for Newtonian fluids in a TC setup were investigated to assess the use of the proposed treatment method as an alternative method in ballast water treatment. The critical Reynolds number values at which the flow undergoes a transition from laminar Couette flow to Taylor vortex flow were determined experimentally by flow visualization and presented through the space-time plots in Fig. 2. In this figure, the evolution of the flow bifurcations can be clearly seen, and the flow patterns characterize the flow regimes. The boundaries between two counter-rotating Taylor vortices are stationary and this can be seen in these observations (Fig. 2). As the rotational rate of the inner cylinder is increased from the rest, the instabilities cause the flow to experience various flow regimes corresponding to several transitions depending on the azimuthal flow velocity and the radius ratio. The flow patterns and the critical Reynolds number values for Newtonian fluids were compared with the experimental results reported by Andereck et al. (1986) and Nemri et al. (2013). The results obtained in this study show good agreement with their results. In the case of a Newtonian fluid, with increasing the inner cylinder speed from the rest, Couette flow was primarily observed at the whole gap in the cylinder at the beginning, and then Circular Couette flow (CCF) with Ekman rolls near the top and bottom of the cylinders was developed at Re=120. As the Reynolds number is increased to a critical value, primary bifurcation, at which the flow is transitioned from CCF to Taylor vortex flow (TVF) appeared at Re=125. The flow patterns were found to be stable in the range of $125 \leq Re < 153$ at this regime. At higher speeds, the flow becomes unstable, and the secondary bifurcation of Wavy Vortex Flow (WVF) transition was observed at Re=153. As the flow state becomes Wavy vortex flow, the vortices deform axially and radially, and become azimuthally wavy. The fluid particles move chaotically and lose their circular motion in this flow state. Akonur and Lueptow (2003) carried out experiments on TC flows and showed that the wavy motion enhanced mixing for a rotating inner cylinder only. The occurrence of traveling waves in WVF enhances fluid exchange between adjacent vortices resulting in more efficient mixing in WVF than in TVF (Nemri et al., 2014). The degree of mixing within the vortices is proportional to the efficiency of separation and filtration. Akonur and Lueptow (2003) also stated that Taylor vortices transport azimuthal momentum radially and axially in Wavy vortex flow. The waviness comes from the jet-like azimuthal velocity profile [25]. The axial particle transport increases with increasing Reynolds number.

The secondary flows that occur after the onset of transition in TC flows have a significant impact on the efficiency of TC-UV reactors because secondary flows generate significantly more circulation and migration between the cylinders than laminar flows. It also affects the durability of UV lamps and light absorbance. Therefore, the accurate determination of the critical point to the transition and the control of the flow structures is important in understanding and then, increasing the TC-UV reactor performance in ballast water treatment.

It is shown in Fig. 3 that the number of emergent vortices and the wavelength of each vortex depends on the radius ratio. The flow structures are usually characterized by both the number of vortices and axial wavelength. For $\eta=0.868$, the axial wavelength and the number of vortices were found to be $\lambda=20.35$ mm (2.14d) and 42, respectively. Whereas in the large gap ($\eta=0.643$), 16 time-independent axisymmetric toroidal

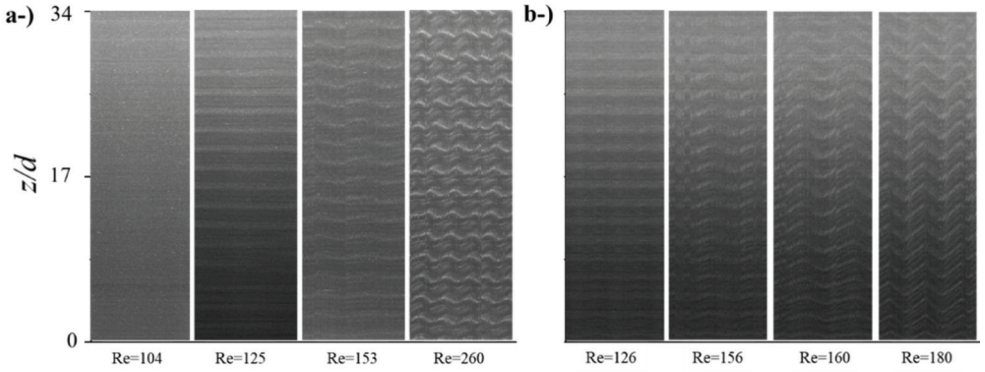

Figure 2. *Space–time Plots of the Various Flow Regimes for the Glycerol Solutions a-) 60% b-) 75%*

vortices by an axial wavelength of λ=50.51 mm (2.02d) were determined. The radius ratio affects the distribution of UV light within the TC reactor system, which is directly proportional to the exposure time. Therefore, the inactivation of *E.coli* is increased with increasing the exposure time and decreasing the gap between the cylinders. The mixing and transportation of microorganisms and suspended solids are expected to be enhanced at higher radius ratio setups compared to the wider gap systems.

Figure 3. *Formation of Taylor Vortices in TVF in Narrow and Wide Gaps*

The inactivation rate constant (k=0.43 $cm^2\ mJ^{-1}$) for *E.coli* used in the present study was obtained from Martínez et al. (2014) [26]. The inactivation of *E. coli* using the TC-UV reactor was compared with that in a conventional UV (C.UV) reactor, and the results are presented in Fig. 4a. It can be seen that significant enhancement in *E. coli* inactivation efficiency is obtained in the TC-UV reactor compared to C.UV reactor. Results show that inactivation of *E. coli* in TC-UV reactor is increased by 36% when compared to C.UV reactor. This increase in efficiency is due to the vortex structures formed in the gap, promoting better mixing and longer contact times. The inactivation of *E. coli* is significantly increased with the Taylor vortices due to migration of microorganisms from the stationary outer wall towards into fast-moving region near the inner wall. The microorganisms and suspended solids will be displaced only within the vortex boundaries, which provide an increase in the exposure time of microorganisms. Moreover, Orlowska et al. (2014) indicated that the inactivation rate was increased by approximately 10-12% when the flow structure was transformed into other flow patterns. The measured inactivation rate values in Orlowska's study was used in the present study to determine the effect of the flow structures on the inactivation of *E. coli*. The inactivation rates of *E. coli* in TVF and WVF are shown in Fig. 4b. This figure clearly shows that the inactivation rate is increased as the flow structure is transitioned to WVF. Although the inactivation efficiency is lower in TVF,

it is seen that it shows better results than the C.UV reactor. Axial and radial mixings are enhanced because of wavy flow, which leads to producing upward and downward vortex deformation and particle exchange. Moreover, the duration of exposure times of UV radiation increases and leading to a slight increase in the efficiency of inactivation of *E. coli*.

The choice of the gap in deciding TC-UV reactor design is a crucial aspect since it influences the disinfection efficiency in the overall process significantly. The velocity and the shear-rate distributions are altered considerably depending on the gap, and consequently, the overall disinfection efficiency is affected. From Fig. 4a it can be seen that the disinfection efficiency of *E.coli* is increased with increasing radius ratio. In the larger gap, the UV light intensity decreases across the gap and thus reducing the inactivation rate of *E. coli.*

Ballast water contains different kinds of harmful bacteria, sediments and suspended solids. Schematic representation of the transportation of these pollutants and the velocity distribution in C.UV and TC-UV reactors is shown in Fig.5. In C.UV reactors, the build-up of a fouling layer that affects the UV radiation efficiency is one of the most serious problems in this type of disinfection processes. The percentage of surviving *E. coli* is increased with decreasing UV radiation efficiency. Moreover, pollutant accumulation on the UV tube surfaces increases energy consumption with more

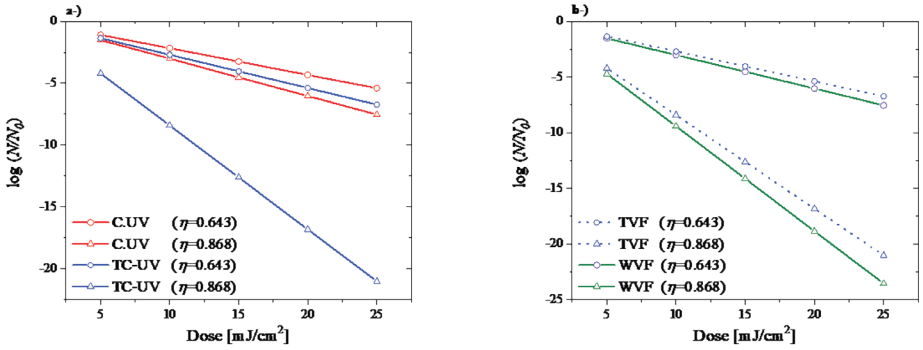

Figure 4. *Inactivation Rates of E. coli a-) in C.UV and TC-UV reactors, b-) at various flow structures in TC-UV*

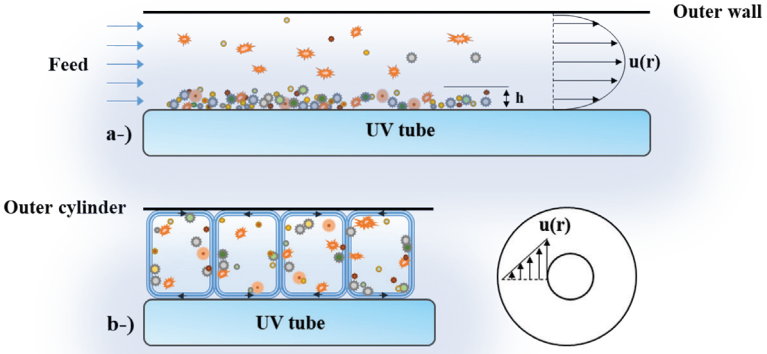

Figure 5. *Schematic Representation of the Transport of Suspended Sediments and Non-native Species in a-) C.UV and b-) TC-UV reactor*

frequent cleaning needs and reduces the lifespan of UV reactors. Whereas, the Taylor vortices emergent in the TC-UV reactor provides a self-cleaning of the tube surface of the inner cylinder. The rotation of the inner cylinder significantly enhances the mass transfer radially and azimuthally within the secondary flows in and between two adjacent vortices. Therefore, TC- UV reactor come into prominence as a ballast water treatment system with higher efficiency.

The influence of the co- and counter-rotating of the outer cylinder on the appearance of the flow structures and the critical Reynolds number was also investigated for a Newtonian fluid. It was observed that the critical values of the Reynolds number and the flow patterns change when the outer cylinder rotates at constant angular velocity. A variety of the flow bifurcations and patterns in the gap has been observed when the cylinders counter-rotate. Spiral vortex flow (SVF), ribbon (RIB) and interpenetrating laminar spiral flow (IPS) structures are observed and shown in space-time plots in Fig.6. Fig. 7 shows the flow regimes map obtained from the visualization experiments which helps understand the effect of the rotating speed and its direction on the flow patterns. From the perspective of the disinfection of harmful bacteria, each flow regime gives information about the flow characteristics, e.g. Couette flow (CCF), Taylor vortex flow (TVF), wavy vortex flow (WVF) and spiral

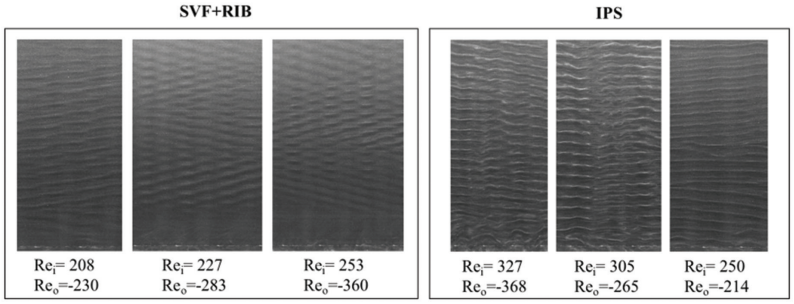

Figure 6. *Emergent Flow Structures in a TC Reactor with Counter-rotating Cylinders*

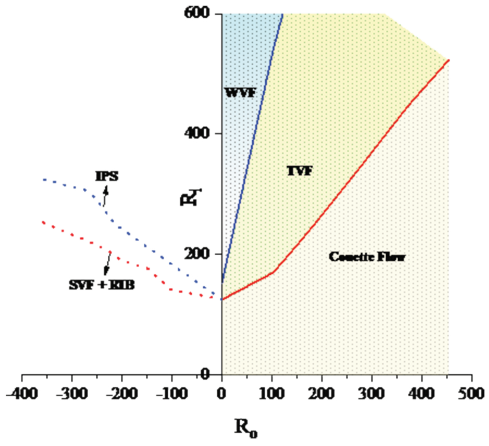

Figure 7. *Critical Transition Boundary Lines of the Various Flow Structures Observed in A Proposed TC-UV Reactor (η=0.868)*

flow. The disinfection efficiency of a TC-UV reactor is directly influenced by the flow pattern within the gap. For example, the occurrence of the WVF structures is associated with the deterioration of a vortex cell and the appearance of flow instabilities. Moreover, these flow patterns increase UV disinfection efficiency due to secondary flow behaviors. Therefore, knowing the flow structure in the gap makes of great practical importance, e.g. contributing to the increase in the inactivation efficiency of non-native species from ballast water.

4. Conclusion

In this study, the critical transition values for various flow patterns in terms of Reynolds number were obtained using glycerol solutions. The effect of radius ratio and the rotation direction of the inner and outer cylinders on the emergent flow patterns were experimentally characterized and compared. The most commonly used treatment process in ballast water treatment is the UV irradiation method. In this study, it is reported that TC-UV treatment unit achieved higher disinfection efficiency comparing to the conventional UV processes for which the results were obtained from the literature. The disinfection efficiency is strongly dependent on the characteristics of the flow structures in TC-UV reactors. Axial and radial mixings are enhanced in TVF and WVF regimes promoting continuous particle migration within the annular gap, i.e. the duration of exposure times of UV radiation increases. The inactivation of *E. coli* in TC-UV reactors with the appearance of the TVF structures is increased by 36% when compared to C.UV reactor. It is also shown that the disinfection efficiency of *E.coli* is increased with increasing radius ratio. The primary objective of this study was to determine the critical transition values of the flow structures which may occur in TC-UV reactors, and provide an excellent basis for further development and evaluation of an alternative UV treatment reactor for the inactivation of non-native species in ballast water. It is reported that TC-UV reactors are promising treatment units protecting the marine environment effectively and efficiently.

References

[1] H. Elcicek, A. Parlak, M. Cakmakci, Effect of Ballast Water on Marine and Coastal Ecology, Journal of Selcuk University Natural and Applied Science. 0 (2013) 454-463–463.

[2] L.A. Drake, M.A. Doblin, F.C. Dobbs, Potential microbial bioinvasions via ships' ballast water, sediment, and biofilm, Marine Pollution Bulletin. 55 (2007) 333–341. https://doi.org/10.1016/j.marpolbul.2006.11.007.

[3] B. Werschkun, S. Banerji, O.C. Basurko, M. David, F. Fuhr, S. Gollasch, T. Grummt, M. Haarich, A.N. Jha, S. Kacan, A. Kehrer, J. Linders, E. Mesbahi, D. Pughiuc, S.D. Richardson, B. Schwarz-Schulz, A. Shah, N. Theobald, U. von Gunten, S. Wieck, T. Höfer, Emerging risks from ballast water treatment: The run-up to the International Ballast Water Management Convention, Chemosphere. 112 (2014) 256–266. https://doi.org/10.1016/j.chemosphere.2014.03.135.

[4] International Maritime Organization (IMO), International Convention for the Control and Management of Ships' Ballast Water and Sediments, London, 2004.

[5] T.D. Waite, J. Kazumi, P.V.Z. Lane, L.L. Farmer, S.G. Smith, S.L. Smith, G. Hitchcock, T.R. Capo, Removal of natural populations of marine plankton by a large-scale ballast water treatment system, Marine Ecology Progress Series. 258 (2003) 51–63. https://doi.org/10.3354/meps258051.

[6] J. Moreno-Andrés, L. Romero-Martínez, A. Acevedo-Merino, E. Nebot, UV-based technologies for marine water disinfection and the application to ballast water: Does salinity interfere with disinfection processes?, Science of The Total Environment. 581–582 (2017) 144–152. https://doi.org/10.1016/j.scitotenv.2016.12.077.

[7] N.B. Petersen, T. Madsen, M.A. Glaring, F.C. Dobbs, N.O.G. Jørgensen, Ballast water treatment and bacteria: Analysis of bacterial activity and diversity after treatment of simulated ballast water by electrochlorination and UV exposure, Science of The Total Environment. 648 (2019) 408–421. https://doi.org/10.1016/j.scitotenv.2018.08.080.

[8] O.-K. Hess-Erga, J. Moreno-Andrés, Ø. Enger, O. Vadstein, Microorganisms in ballast water: Disinfection, community dynamics, and implications for management, Science of The Total Environment. 657 (2019) 704–716. https://doi.org/10.1016/j.scitotenv.2018.12.004.

[9] D. Wu, H. You, R. Zhang, C. Chen, D.-J. Lee, Ballast waters treatment using UV/Ag–TiO2+O3 advanced oxidation process with Escherichia coli and Vibrio alginolyticus as indicator microorganisms, Chemical Engineering Journal. 174 (2011) 714–718. https://doi.org/10.1016/j.cej.2011.09.087.

[10] O. Casas-Monroy, R.D. Linley, P.-S. Chan, J. Kydd, J. Vanden Byllaardt, S. Bailey, Evaluating efficacy of filtration+UV-C radiation for ballast water treatment at different temperatures, Journal of Sea Research. 133 (2018) 20–28. https://doi.org/10.1016/j.seares.2017.02.001.

[11] Z. Lu, K. Zhang, Y. Shi, Y. Huang, X. Wang, Efficient Removal of Escherichia coli from Ballast Water Using a Combined High-Gradient Magnetic Separation-Ultraviolet Photocatalysis (HGMS-UV/TiO2) System, Water Air Soil Pollut. 229 (2018) 243. https://doi.org/10.1007/s11270-018-3902-2.

[12] Y.J. Jung, Y. Yoon, T.S. Pyo, S.-T. Lee, K. Shin, J.-W. Kang, Evaluation of disinfection efficacy and chemical formation using MPUV ballast water treatment system (GloEn-PatrolTM), Environmental Technology. 33 (2012) 1953–1961. https://doi.org/10.1080/09593330.2012.655315.

[13] L.J. Forney, Z. Ye, T. Koutchma, UV Disinfection of E. coli Between Concentric Cylinders: Effects of the Boundary Layer and a Wavy Wall, Ozone: Science & Engineering. 30 (2008) 405–412. https://doi.org/10.1080/01919510802473872.

[14] L.J. Forney, C.F. Goodridge, J.A. Pierson, Ultraviolet Disinfection: Similitude in Taylor–Couette and Channel Flow, Environ. Sci. Technol. 37 (2003) 5015–5020. https://doi.org/10.1021/es0303236.

[15] Z. Ye, L.J. Forney, T. Koutchma, A.T. Giorges, J.A. Pierson, Optimum UV Disinfection between Concentric Cylinders, Ind. Eng. Chem. Res. 47 (2008) 3444–3452. https://doi.org/10.1021/ie0703641.

[16] L.J. Forney, J.A. Pierson, Z. Ye, Juice irradiation with Taylor-Couette flow: UV inactivation of Escherichia coli, J. Food Prot. 67 (2004) 2410–2415. https://doi.org/10.4315/0362-028x-67.11.2410.

[17] F. Crapulli, Disinfection and advanced oxidation of highly absorbing fluids by UV/VUV light: process modeling and validation, Electronic Thesis and Dissertation Repository. (2015). https://ir.lib.uwo.ca/etd/2753.

[18] S.T. Wereley, A. Akonur, R.M. Lueptow, Particle–fluid velocities and fouling in rotating filtration of a suspension, Journal of Membrane Science. 209 (2002) 469–484. https://doi.org/10.1016/S0376-7388(02)00365-4.

[19] C.D. Andereck, S.S. Liu, H.L. Swinney, Flow regimes in a circular Couette system with independently rotating cylinders, Journal of Fluid Mechanics. 164 (1986) 155–183. https://doi.org/10.1017/S0022112086002513.

[20] Murray Rudman, Mixing and Particle Dispersion in the Wavy Vortex Regime of Taylor-Couette Flow, AICHE Journal. 44 (n.d.) 1015–1026.

[21] S.T. Wereley, R.M. Lueptow, Spatio-temporal character of non-wavy and wavy Taylor–Couette flow, Journal of Fluid Mechanics. 364 (1998) 59–80. https://doi.org/10.1017/S0022112098008969.

[22] E. Dluska, J. Wolinski, S. Wronski, Toward Understanding of Two-Phase Eccentric Helical Reactor Performance, Chemical Engineering & Technology. 28 (2005) 1016–1021. https://doi.org/10.1002/ceat.200500140.

[23] M. Orlowska, T. Koutchma, M. Kostrzynska, J. Tang, C. Defelice, Evaluation of mixing flow conditions to inactivate Escherichia coli in opaque liquids using pilot-scale Taylor–Couette UV unit, Journal of Food Engineering. 120 (2014) 100–109. https://doi.org/10.1016/j.jfoodeng.2013.07.020.

[24] Z. Ye, L.J. Forney, T. Koutchma, A.T. Giorges, J.A. Pierson, Optimum UV Disinfection between Concentric Cylinders, Ind. Eng. Chem. Res. 47 (2008) 3444–3452. https://doi.org/10.1021/ie0703641.

[25] A. Akonur, R.M. Lueptow, Three-dimensional velocity field for wavy Taylor–Couette flow, Physics of Fluids. 15 (2003) 947–960. https://doi.org/10.1063/1.1556615.

[26] L. Romero-Martínez, J. Moreno-Andrés, A. Acevedo-Merino, E. Nebot, Improvement of ballast water disinfection using a photocatalytic (UV-C + TiO2) flow-through reactor for saltwater treatment, Journal of Chemical Technology & Biotechnology. 89 (2014) 1203–1210. https://doi.org/10.1002/jctb.4385.